



Effect of biasing on divertors in low and high ionization states

H. Matsuura^{*}, T. Yamamoto, M. Numano

Osaka Prefecture University, Gakuen-cho 1-1, Sakai, Osaka 599-8531, Japan

Abstract

One-dimensional transport equations were used to study the biased divertor plasma. By including ionization processes, a drastic transition between low and high ionization states was found. In high ionization state, the heat flux at the positively biased divertor leg increases mainly due to Sebeck effect. The temperature can be controlled with the biasing only in this state. Momentum loss due to charge exchange processes prevented the transition to the high ionization state. © 2001 Elsevier Science B.V. All rights reserved.

Keywords: Plasma properties

1. Introduction

In order to control the divertor plasma, the divertor biasing has been tested on medium-size Tokamaks such as DIII-D and JFT-2M. Various simulation models have been developed to analyze how plasma parameters will change with the biasing [1–3]. In these studies, however, some important physical effects were not considered for simplicity. For example, plasma temperature was not calculated in [1]. The Seebeck effect and the heat loss in the divertors are not taken into account and neutral ionization was not calculated in the study of [2]. Plasma momentum loss in the divertors is neglected in [3].

In order to protect wall materials from large heat flux, the so-called detached plasma is important. In this plasma, heat and momentum losses due to the interaction with neutrals become larger in the divertor plasma. Therefore it is necessary to study the effect of the biasing on the divertor plasma where ionization and charge exchange of neutrals are dominant.

In Section 2, we explain our calculation model, which includes the interaction of plasma with neutral particles. In Section 3, we present some calculated results. Section

4 explains why plasma current may flow in the opposite direction to applied bias voltage in a high ionization condition. Section 5 is the summary.

2. Model and equations

2.1. Modeling of the biased plasma

In this paper, we use a simple one-dimensional geometry along the divertor field line. Two divertor plates terminate the field line and an external circuit connects them. We distinguish the plasma parameters near the two plates with the subscripts ‘1’ and ‘2’. The heat and particle sources from the main plasma are located at the stagnation point, which is referred with the subscript ‘0’. All physical values in this subsection are normalized with values given in Table 1, where typical values are calculated for H-plasma with particle loss from main plasma of $\Gamma_0 = 2.0 \times 10^{22}$ 1/m²s and heat loss of $q_0 = 1.0 \times 10^7$ W/m².

We use particle, momentum, energy, and charge conservation equations with integrated Fourier’s law for two divertor regions, the relation between the ionization probability and flux amplification factor, and Ohm’s law. By solving the following nine simultaneously, divertor densities (n_1, n_2), temperatures (T_1, T_2), non-dimensional potentials ($\phi_1 = e\Phi_1/T_1, \phi_2 = e\Phi_2/T_2$), flux amplification factors (R_1, R_2), and a stagnation point temperature (T_0) are derived.

^{*} Corresponding author. Tel.: +81-722 54 9226; fax: +81-722 59 3340.

E-mail address: matsu@energy.osakafu-u.ac.jp (H. Matsuura).

Table 1
Normalized constants of plasma parameters

Physical parameter	Unit	Definition	Typical value
Particle flux	$1/\text{m}^2\text{s}$	$\Gamma_n = \frac{1}{2}\Gamma_0$	1.0×10^{22}
Heat flux	W/m^2	$q_n = \frac{1}{2}q_0$	0.5×10^7
Current density	A/m^2	$J_n = e\Gamma_n$	1.60×10^3
Temperature	J	$T_n = \frac{q_n}{\Gamma_n f(\phi_0)}$	7.70×10^{-17}
Density	$1/\text{m}^3$	$n_n = \sqrt{\frac{m_i}{2T_n}}\Gamma_n$	3.30×10^{16}
Divertor length	m	$L_n = \frac{2k_B(T_n)T_n}{7q_n}$	1.06×10^5
Potential	V	$V_n = \frac{T_n}{e}$	4.81×10^2
Electric resistivity	Ωm	$(\eta_e)_n = \frac{2}{7} \frac{V_n}{J_n L_n}$	8.08×10^{-7}
Seebeck coefficient		$(\alpha_T)_n = f(\phi_0)$	6.49
Heat transition factor		$(f(\phi))_n = f(\phi_0)$	6.49

- Charge conservation

$$\sum_{j=1}^2 n_j T_j^{1/2} g(\phi_j) = 0. \quad (1)$$

- Energy conservation

$$\sum_{j=1}^2 n_j T_j^{3/2} f(\phi_j) = 2 - \Delta E \sum_{j=1}^2 n_j T_j^{1/2} \eta_j - \sum_{j=1}^2 2n_j T_j^{3/2} \xi_j. \quad (2)$$

- Relation between the ionization probability and flux amplification factor

$$R_j = \frac{1}{1 - \eta_j} \quad (j = 1, 2). \quad (3)$$

- Particle conservation

$$\sum_{j=1}^2 \frac{n_j T_j^{1/2}}{R_j} = 2. \quad (4)$$

- Momentum conservation

$$n_1 T_1 (1 + \xi_1) = n_2 T_2 (1 + \xi_2). \quad (5)$$

- Integrated Fourier's law

$$n_j T_j^{3/2} f(\phi_j) L_j = D(T_j, T_0, \phi_j) \quad (j = 1, 2). \quad (6)$$

- Ohm's law

$$V_{\text{ext}} = (\phi_1 T_1 - \phi_2 T_2) + \gamma(T_1 - T_2) + (E(T_1, T_0, \phi_1) - E(T_2, T_0, \phi_2)), \quad (7)$$

where η and ξ are the ionization probability and the drag factor of the neutral, which are explained in Section 2.2, ΔE is energy loss per ionization. We assume that ΔE is larger than the hydrogen ionization energy (13.6 eV) due to existence of the excitation process and impurities. $\gamma = \gamma_p - \alpha_T$ represents the presheath effect (γ_p) and the thermo-electric effect (α_T). $\Gamma = nT^{1/2}$, $J = nT^{1/2}g(\phi)$, and $Q = nT^{3/2}f(\phi)$ are the divertor flux densities of particle, current and heat. $g(\phi)$ and $f(\phi)$ are defined as the following:

$$g(\phi) = 1 - \exp(\phi_0 - \phi), \quad (8)$$

$$f(\phi) = 2 + \phi + 2\sqrt{\frac{m_i}{4\pi m_e}} \exp(-\phi), \quad (9)$$

where $\phi_0 (= \log\{\sqrt{(m_i/4\pi m_e)}(1 - \gamma_e)\})$ is the floating potential, m_i and m_e the ion and electron masses, γ_e is the secondary electron emission coefficient of the divertor plate (set to be 0 now). L is the length of divertor (that is the distance between a stagnation point and a divertor plate).

Using the classical transport coefficient (thermal conductivity $\kappa \propto T^{5/2}$ and electrical conductivity $\sigma \propto T^{3/2}$), Functions D and E are calculated as the following:

$$D(T, T_0, \phi) = -\frac{7}{2} \int_{T_0}^T \frac{x^{5/2}}{1 + sx} dx, \quad (10)$$

$$E(T, T_0, \phi) = \frac{\eta_e g(\phi)}{Tf(\phi)} \int_{T_0}^T \frac{x}{1 + sx} dx, \quad (11)$$

where $s = \alpha_T J / q = \alpha_T g(\phi) / Tf(\phi)$, $\eta_e = \kappa / T\sigma$.

2.2. Interaction model with neutral particles

The neutral ionization probability (η) for the divertor with the length of L was calculated in [4] with a simple analytic formula. For the detached plasma modeling, momentum loss by the charge exchange process seems to be important. So we extended this formula and employed another formula for the neutral 'drag factor (ξ)' due to the charge exchange. Velocity and temperature of neutrals were neglected compared with those of the plasma in calculation of the right-hand side of Eq. (2) with η and ξ . Neutral velocity was also neglected in calculation of ξ itself by Eq. (13).

- Ionization probability

$$\eta = \frac{1}{\Gamma} \int_0^L nn_n \langle \sigma v \rangle_{\text{ion}} dz = \frac{\lambda}{\lambda_{\text{ion}}} (1 - f_p e^{-b/\lambda}) (1 - e^{-L/\lambda}). \quad (12)$$

- Neutral drag factor

$$\begin{aligned}\xi &= \frac{-1}{4nT} \int_0^L (-m_i u + m_n u_n) n n_n \langle \sigma v \rangle_{cx} dz \\ &= \frac{1}{2} \frac{\lambda}{\lambda_{cx}} (1 - f_p e^{-b/\lambda}) (1 - e^{-L/\lambda}).\end{aligned}\quad (13)$$

In Eqs. (12) and (13), the neutral density is assumed to decay exponentially from the divertor plate ($= n_{n0} e^{-z/\lambda}$), and the recycled neutral flux is estimated as $\Gamma_{n0}/\Gamma = (1 - f_p e^{-b/\lambda})$, where f_p is the effective pumping factor (set to be 0.05) and b is the divertor width (set to be 0.05 m). λ is the total mean free path,

$$\frac{1}{\lambda} = \frac{1}{\lambda_{cx}} + \frac{1}{\lambda_{ion}} \quad (14)$$

and λ_{ion} and λ_{cx} are the mean free paths of ionization and charge exchange, respectively,

$$\lambda_{ion} = \frac{u}{n \langle \sigma v \rangle_{ion}}, \quad \lambda_{cx} = \frac{u}{n \langle \sigma v \rangle_{cx}}, \quad (15)$$

where, the ionization rate coefficient $\langle \sigma v \rangle_{ion}$ is calculated by Verner's routine [5,6] and the charge exchange rate coefficient $\langle \sigma v \rangle_{cx}$ is obtained by integrating Rivière's formula [7]. Divertor plasma asymmetry, which has often been observed experimentally, can be introduced into our model by changing the length between two divertors. In this paper, however, we concentrate our study to the case of $L_1 = L_2 = L_s$ to see the effect of the divertor biasing more clearly.

3. Calculation results

3.1. Seebeck effect

Firstly, we find that the current induced by the biasing plays a very important roll in controlling the heat flux (Seebeck effect [8]). In [2], α_T was set to be 0 and the auxiliary functions of Eqs. (6) and (7) were $D = T_0^{\frac{7}{2}} - T^{\frac{7}{2}}$ and $E \sim T_0^2 - T^2$, resulting that heat flux was constant with varying the bias voltage V_{ext} . In order to compare with this result, we increase Seebeck coefficient α_T from zero to the value (0.71) for hydrogen ions, keeping that $\eta = 0.9$ and $\xi = 0$. In $\alpha_T = 0.71$ case, heat flux Q_1 and temperature T_1 increase with positive V_{ext} , though Q_1 is constant and T_1 decreases in $\alpha_T = 0$ case.

3.2. Transition between low and high ionization states

Next, we change the length of divertor (L_s) and calculate also ionization probability (η), keeping that $\xi = 0$. When L_s becomes longer, a very sharp transition of ionization probability (η) to a higher value is observed and vice versa. At the same time, the plasma

Symmetric temp. for Delta E = 80[eV]

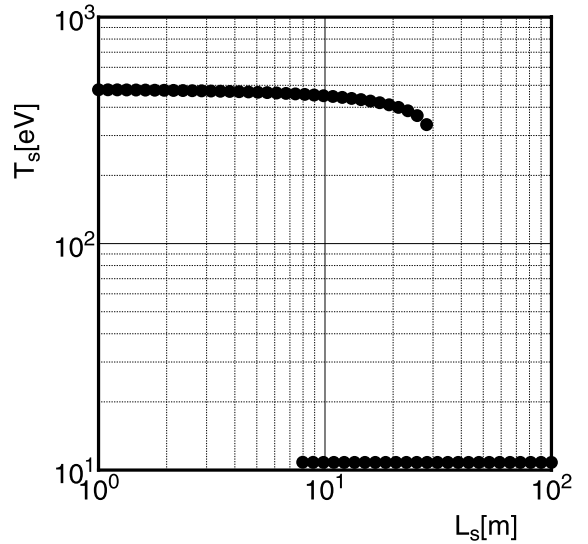


Fig. 1. Divertor temperature T_s for $V_{ext} = 0$ as the function of divertor length L_s is shown. Energy loss per ionization is set to be 13.6 and 80.0 eV.

parameters also show hysteresis curve. One example is given in Fig. 1. The horizontal axis is L_s and the vertical axis is the symmetric temperature T_s for $V_{ext} = 0$, which is called 'symmetric' because two divertor legs are of the same length and both temperatures are equal. As ΔE is the energy loss per ionization, T_s for the low ionization state does not depend on ΔE (400–500 eV in this case). The high ionization state is restricted to larger L_s with increasing ΔE and the temperature T_s for this state decreases.

The effect of the divertor biasing on the plasma parameters appears quite different between low and high ionization states. It is shown in Fig. 2 that the current J_1 increases with V_{ext} in the low ionization divertor whereas it decreases in the high ionization divertor. The heat flux shows a similar reversing between low and high ionization divertors. It was more difficult to control plasma parameters with the biasing in the low ionization state. The neutral ionization probability η itself is hardly affected with the biasing in both states. This means that the biasing has no effect on the neutral behavior.

A change of the main plasma heat/particle loss can trigger this ionization transition. So a kind of instability might develop in the biased divertor plasma.

3.3. Charge exchange effect

When we include the charge exchange (i.e., ξ) calculation, the ionization probability η_s generally drops. As shown in Fig. 3, it is difficult to obtain the high

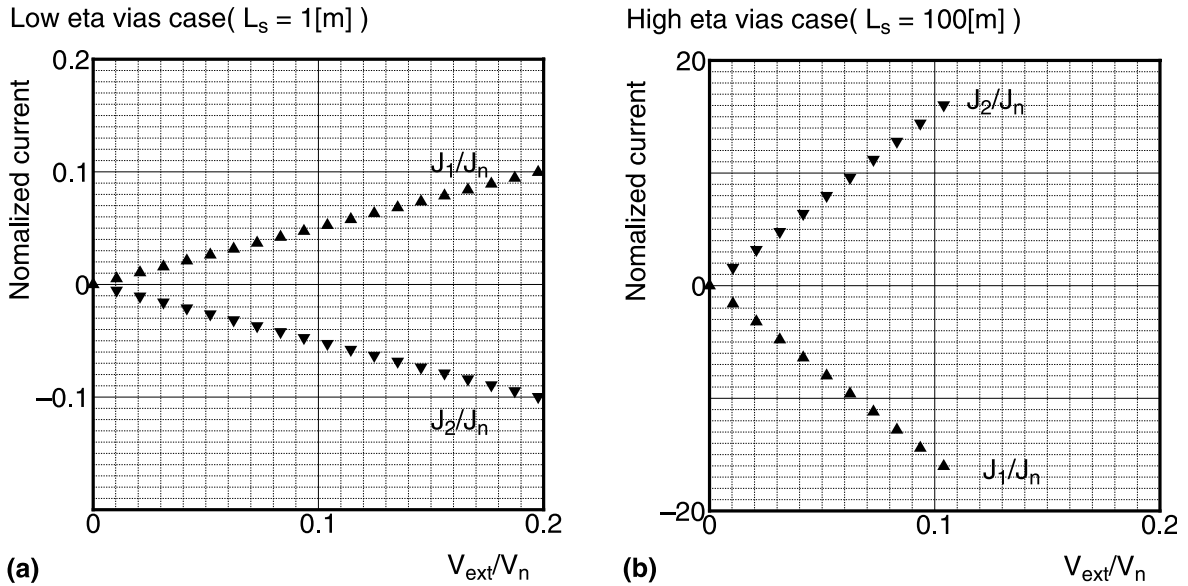


Fig. 2. Normalized current as the function of the normalized bias voltage V_{ext}/V_n is shown.

ionization state even at large divertor length L_s . In this case, η_s for $L_s = 100$ m changes from 0.95 (in the wo/CX case) to 0.14 (in the w/CX case). ξ_s (in the w/CX case) is ~ 0.3 and less dependent on L_s .

Fig. 3 shows that charge exchange processes dominate the plasma even for long divertor length, where one

would normally expect detached plasma. The particle flux amplification due to ionization is suppressed and plasma control with the divertor biasing is also expected to be difficult.

4. Discussion

As shown in Fig. 2, the current in the high ionization state flows in the opposite direction of the bias voltage polarity. We discuss it briefly here.

Three terms in the Ohm's law (7) are shown in Fig. 4 as function of the bias voltage V_{ext} . In the low ionization case, the temperatures of two divertors are almost equal ($T_1 = T_2$). So thermo-electronic effect (and presheath effect) $\gamma(T_1 - T_2)$ is small (T-term in the figure). Joule loss $E(T_1, T_0, \phi_1) - E(T_2, T_0, \phi_2)$ is also negligible (J-term). As the current is proportional to $g(\phi) \sim \phi - \phi_0$, external applied V_{ext} drives the current in the co-direction.

In the high ionization case, the Joule losses term is very large and the potential difference in the plasma (P-term, $T_1\phi_1 - T_2\phi_2$) is only about 10% of V_{ext} . Moreover, as $T_1 > T_2$ for positive V_{ext} , $\phi_1 < \phi_0 < \phi_2$. So V_{ext} drives the current in the counter-direction.

5. Summary

We used one-dimensional plasma transport equations including the interaction with neutral particles and obtained the following results.

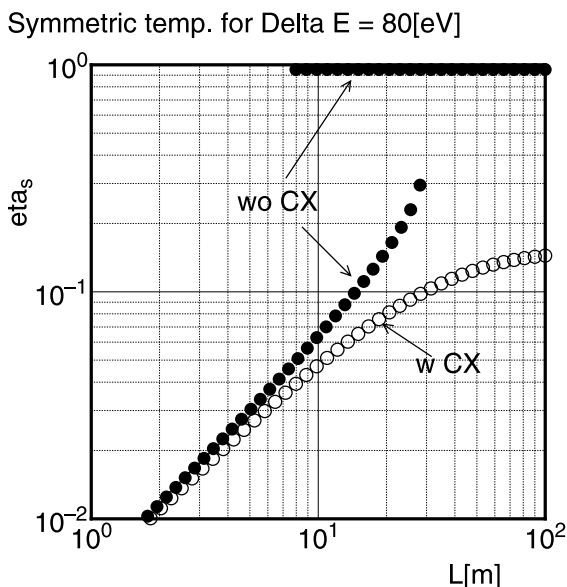
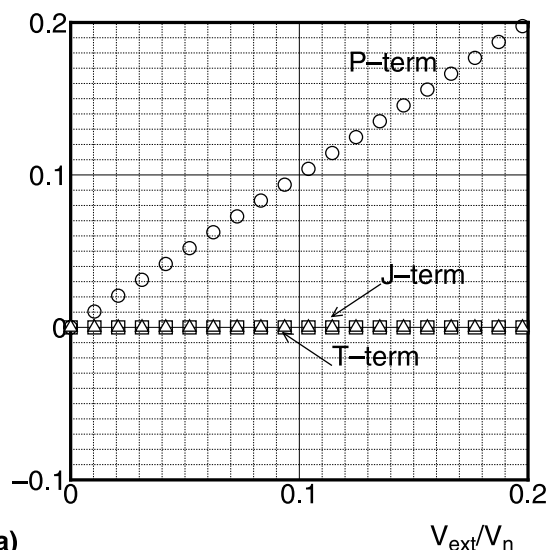
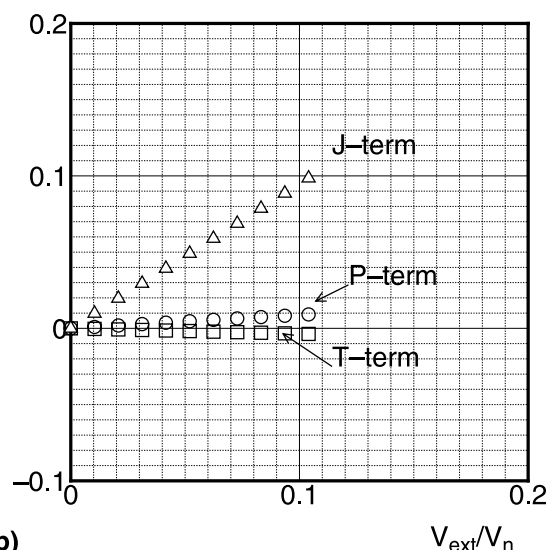


Fig. 3. Charge exchange effect on ionization probability η_s for $\Delta E = 80.0$ eV. Closed circles are the data without charge exchange calculation. Open circles are the data with the charge exchange calculation.

Terms in the Ohm's law($L_s = 1[m]$)

(a)

Terms in the Ohm's law($L_s = 100[m]$)

(b)

Fig. 4. Magnitude of three terms of Ohm's law are compared as the function of the normalized bias voltage V_{ext}/V_n for low and high ionization states.

- The Seebeck effect, which had often been omitted due to simplicity in previous works, was very important in controlling the heat flux with the biasing.
- As the length of the divertor was increased, the ionization probability of neutral particles and plasma particle flux amplification factor jumped from the low value (low ionization state) to the high value (high ionization state). This transition showed a hysteresis property.
- The response of divertor plasma parameters to the application of the external bias voltage was quite different in the low and high ionization states. It was more difficult to control the plasma with the biasing in the low ionization state.
- Including the charge exchange effect, we found it difficult to obtain the high ionization state. So detached plasma control with the divertor biasing is also expected to be difficult.
- In the high ionization state the current flowed along opposite direction of bias voltage polarity. This was explained with the fact that the plasma temperature dropped toward divertor plates and that a non-dimensional potential decreased.

Acknowledgements

We thank Dr. Dima Verner of the university of Kentucky for providing useful subroutines to calculate various atomic reaction rates.

References

- [1] G.M. Staebler, F.L. Hinton, Nucl. Fus. 29 (1989) 1820.
- [2] K. Nagasaki, NIFS-79, 1991.
- [3] N. Hayashi, T. Takizuka et al., Nucl. Fus. 38 (1998) 1695.
- [4] S. Saito et al., Nucl. Fus. 25 (1985) 828.
- [5] Dima Verner, private communication. (<ftp://gradj.pa.uky.edu/dima/col/colfit.f>).
- [6] G.S. Voronor, Atomic Data Nucl. Data Tables 65 (1997) 1.
- [7] D.L. Galbraith et al., Nucl. Fus. 19 (1979) 1047.
- [8] F.L. Hinton, Handbook of Plasma Physics, vol. 1, North-Holland, Amsterdam, 1983, p. 183.